Geophysical Research Letters

RESEARCH LETTER
10.1029/2018GL077316

Key Points:
- The correlation between CO_2 seasonal cycle amplitude and temperature became negative around the year 2000 at most northern stations
- The positive spring net biome productivity-temperature correlation has been weakening since the mid-1990s
- The negative autumn/winter net biome productivity-temperature correlation has diminished in the mid-to-high latitudes since the early-2000s

Supporting Information:
- Supporting Information S1

Correspondence to:
Y. Yin,
yiyin@caltech.edu

Citation:
Yin, Y., Ciais, P., Chevallier, F., Li, W., Bastos, A., Piao, S., et al. (2018). Changes in the response of the Northern Hemisphere carbon uptake to temperature over the last three decades. *Geophysical Research Letters*, *45*, 4371–4380. https://doi.org/10.1029/2018GL077316

Received 29 JAN 2018
Accepted 7 APR 2018
Accepted article online 19 APR 2018
Published online 4 MAY 2018

Changes in the Response of the Northern Hemisphere Carbon Uptake to Temperature Over the Last Three Decades

Yi Yin[1,2], Philippe Ciais[2], Frederic Chevallier[2], Wei Li[2], Ana Bastos[2,3], Shilong Piao[4,5], Tao Wang[5], and Hongyan Liu[4]

[1]California Institute of Technology, Pasadena, CA, USA, [2]Laboratoire des Sciences du Climat et de l'Environnement, CEA-CNRS-UVSQ, Gif-sur-Yvette, France, [3]Now at Dept Geography, Ludwig Maximilians Universität, München, Germany, [4]Department of Ecology, College of Urban and Environmental Sciences, Peking University, Beijing, China, [5]Key Laboratory of Alpine Ecology and Biodiversity, Institute of Tibetan Plateau Research, Chinese Academy of Sciences, Beijing, China

Abstract The CO_2 seasonal cycle amplitude (SCA) in the Northern Hemisphere has increased since the 1960s—a feature attributed mainly to enhanced vegetation activity along climate warming and CO_2 increase. We identified a temporal change in the sign of the correlation between SCA and air temperature (T) from positive to negative around the year 2000 at most Northern Hemisphere ground stations, consistent with signals from satellite column CO_2 measurements since the mid-2000s. Further, we explored potential causes of this change using net biome productivity estimates from three atmospheric inversions for the period 1980–2015. The change in the SCA-T relationship is primarily attributable to changes in the net biome productivity-T relationship: positive correlations weakened in the spring in the high latitudes, confirming a limit to the "warmer spring-bigger carbon sink" mechanism; negative correlations diminished in the autumn/winter in the mid-to-high latitudes, challenging the "warmer winter-larger carbon release" assumption and highlighting the complexity of carbon processes outside the peak growing season.

Plain Language Summary The seasonal cycle amplitude (SCA) of atmospheric CO_2—an integrated signal of the terrestrial ecosystem metabolism—has increased since the 1960s in the Northern Hemisphere, a feature attributed mainly to enhanced vegetation activity along climate warming and CO_2 increase. Earlier studies suggest a strong positive year-to-year correlation between SCA and air temperature (T). Here we identified a temporal change in the sign of the SCA-T correlation from positive to negative around the year 2000 at most Northern Hemisphere ground stations, consistent with signals from satellite column CO_2 observations. We further explored potential causes of this change using land carbon flux (termed as net biome productivity) estimates from three atmospheric inversions for the period 1980–2015. The change in the SCA-T relationship is primarily attributable to changes in the net biome productivity-T relationship: positive correlations weakened in the spring in the high latitudes, confirming a limit to the "warmer spring-bigger carbon sink" mechanism; negative correlations diminished in the autumn/winter in the mid-to-high latitudes, challenging the "warmer winter-larger carbon release" assumption. This finding highlights a dynamic temperature sensitivity of the terrestrial ecosystem to climate warming and cautions the use of current carbon-climate response to constrain future projections.

1. Introduction

The atmospheric concentration of carbon dioxide (CO_2) in the Northern Hemisphere (NH) oscillates over the year, primarily controlled by the imbalance between the vegetation photosynthetic CO_2 uptake and the release of CO_2 from the decomposition of the litter and soil organic matter and fire disturbance. The seasonal cycle amplitude (SCA) of atmospheric CO_2—an integrated signal of the terrestrial ecosystem metabolism—has increased since the 1960s (Keeling et al., 1996), most significantly in regions north of 45°N where an increase of 50% has occurred at altitudes of 3 to 6 km over the last 50 years (Graven et al., 2013). Many studies have analyzed the drivers of this SCA increase and identified factors associated with enhanced photosynthetic uptake in the midlatitude and high latitude, for example, climate warming, a lengthening growing season, CO_2 fertilization, and nitrogen deposition (Forkel et al., 2016; Graven et al., 2013; Keeling et al., 1996; Randerson et al., 1997; Zhu et al., 2016), while a fraction of this enhanced uptake is released back to the atmosphere during the nongrowing season (Piao et al., 2008; Piao, Liu, Wang, Ciais, et al., 2017).

Superimposed on the long-term increasing trend, the interannual variations (IAV) of SCA at the northern measurement stations are also large (e.g., Barrow, Alaska, ~8% IAV versus ~0.6% year trend) but less well understood. On a quasi-decadal scale, Keeling et al. (1996) found a positive correlation between the SCA (at Barrow and Mauna Loa) and the NH land temperature (T, 30–80°N) for the period 1960–1995. Based on several other NH stations over the period 1980–1997, Randerson et al. (1999) found a strong positive year-to-year correlation between the spring T and the early season carbon uptake and between the fall T and the late season carbon release. This finding is consistent with warmer years enhancing growing season CO_2 uptake and nongrowing season CO_2 release, and thus resulting in larger SCA. In contrast, an anticorrelation between SCA and T was found for a more recent period (2003–2012) by Schneising et al. (2014) using satellite retrievals of the column-average dry air mole fraction of CO_2 (noted as X_{CO2} hereafter) from the SCanning Imaging Absorption spectroMeter for Atmospheric CHartographY (SCIAMACHY) and from equivalent X_{CO2} simulated using the CarbonTracker CO_2 reanalysis based on in situ CO_2 surface measurements (Peters et al., 2007).

As the signs of the correlations between these studies were obtained for different periods (pre-2000 versus post-2000), it is possible that temporal change in the sign of the correlations between SCA and T between these two decades occurred. However, the results of Schneising et al. (2014) are not directly comparable with the surface observations, as their results based on the CarbonTracker reanalysis, although informed by surface measurements, bear the temporal and spatial sampling of the SCIAMACHY and its prior information. In situ observations are sampled near the surface from a sparse network with most sites being in the marine boundary layer, while satellite data integrate CO_2 vertically over the air column and sample the interior of the continents with considerably denser spatial coverage. Temporally, in situ data have a high measurement frequency and cover all seasons and all weather conditions throughout the year. In contrast, satellite such as SCIAMACHY that relies on reflected sunlight is limited to cloud-free conditions and has reduced coverage in the high latitudes between the autumn to the spring equinox under high solar zenith angle ($>$70°).

To understand the various results regarding the SCA-T correlations, we revisit the temporal changes in the year-to-year correlation between SCA and T using both surface CO_2 observations from NH stations—that have relatively long records—and satellite X_{CO2} measurements—that provide dense spatial sampling of the continental interior—in a consistent manner. To further untangle factors that could have contributed to the changes in SCA–T correlation, we also investigate changes in the correlations between the NH terrestrial carbon uptake and temperature in different seasons using spatial and temporally resolved net biome productivity (NBP) estimates from atmospheric inversions for the period 1980–2015.

2. Materials and Methods

2.1. Atmospheric CO_2 Concentration and the Analysis of SCA

We include measurements of surface CO_2 dry mole fraction from 16 stations of the National Oceanic and Atmospheric Administration/Earth System Research Laboratory/Global Monitoring Division cooperative global air sampling network located north of 30°N and with records longer than 20 years (station distribution is shown in Figure S1; Dlugokencky et al., 2017). The longest record is from the Barrow station, covering the period from 1973 to 2015 after excluding discontinuous sampling in the late 1960s. CO_2 signals detected at Barrow are influenced by carbon fluxes from both the high latitudes and the midlatitudes through atmospheric transport and mixing (Liu, Wang, Ciais, et al., 2017). Previous studies suggested that the major contribution to the CO_2 seasonal cycle is from boreal (~35%) and arctic (~35%) ecosystems, while the temperate and the subtropical regions contribute ~30% (Graven et al., 2013). A similar magnitude of the relative latitudinal contributions was also found based on the vertical CO_2 gradient over Alaska, where ~41% of the SCA is influenced by long-range transport from mid-to-low latitudes (Parazoo et al., 2016). Hence, when analyzing the Barrow SCA-T correlations, we consider both the high latitude and midlatitude temperature variations.

We also use satellite retrievals of X_{CO2} from two instruments—SCIAMACHY and GOSAT (Greenhouse Gases Observing SATellite). SCIAMACHY data cover the period from August 2002 to April 2012, with a spatial resolution of ~30 × 60 km^2. Here we use the CRDP4/BESD retrievals, which is the most up-to-date SCIAMACHY X_{CO2} product using the European Space Agency Greenhouse Gases-Climate Change Initiative baseline algorithm, but different from that used by Schneising et al. (2014) (http://www.esa-ghg-cci.org/sites/default/files/

documents/public/documents/GHG-CCI_DATA.html, Reuter et al., 2011). The GOSAT data extend the SCIAMACHY record and cover the period from April 2009 to December 2015, with a spatial resolution of ~10 × 10 km^2; we used the CRDP4/OCFP retrievals (Cogan et al., 2012). Valid measurements were averaged at a monthly time step into 1 × 1 degree^2 bins before further analysis. Note again that the coverage of satellite observations is limited to cloud-free scenes, and no measurements over the northern high latitudes are available from autumn to spring equinoxes. Further analysis assumes that these sampling factors do not induce systematic errors in the estimates of SCA interannual variations using spatially averaged X_{CO2}.

We filter the surface observations to remove outliers that differ from the monthly means by more than three times the standard deviations of all the observations in that month to reduce local signals. The filtered surface observations and the regionally averaged X_{CO2} time series are then processed following the steps below to estimate the SCA (https://www.esrl.noaa.gov/gmd/ccgg/mbl/crvfit/crvfit.html; Thoning et al., 1989):

1. Fit the observational time series with a quadratic polynomial for the trend and four harmonics for the seasonal variations (equation (1))

$$f(t) = a_0 + a_1 t + a_2 t^2 + \sum_{n=1}^{4} [C_n \sin(2n\pi t) + D_n \cos(2n\pi t)] \quad (1)$$

where t is the decimal year (normalized to represent the seasonal component); a_0, a_1, and a_2 are coefficients for the offset, the linear, and quadratic terms, respectively; C_n and D_n are coefficients for the amplitude of seasonal variations; and n is the number of harmonics.

2. Apply two low-pass filters to the residue of the functional fit with 150- and 667-day cutoffs to define short-term variations that are not represented by equation (1). The filtered data are added back to the polynomial terms to generate a smooth long-term trend. The seasonal cycles are then estimated by removing the long-term trend from the monthly mean values, and SCA are derived as the difference between the annual maximum and the minimum.

2.2. Carbon Fluxes From Atmospheric Inversions

We include here atmospheric inversion NBP products covering the period 1980–2015 from two independent inversion systems: the Copernicus Atmosphere Monitoring Service (CAMS) inversion system (http://atmosphere.copernicus.eu/; Chevallier et al., 2010) and the JENA CarboScope inversion system (http://www.bgc-jena.mpg.de/CarboScope/; Rödenbeck et al., 2003). While both inversions provide gridded posterior NBP fluxes estimated by assimilating surface measurements and both are guided by the ERA-Interim meteorological reanalysis, the two inversion systems differ significantly in many aspects including the prior information and its error structures, the atmospheric transport model, and the observations being assimilated (see more details in the reference above). For the CAMS, we use v15r4, which assimilates an increasing number of stations over time from 1979 to early 2016 as more stations became available (in total 133 sites with records longer than five years, the yearly distributions of stations are shown in Chevallier, 2016). This approach makes maximum usage of available measurements, but it implies a variable spatial constraint on the inversion in time. CAMS_v15r4 has a spatial resolution of 1.875° × 3.75° with weekly optimized posterior fluxes.

In contrast, the JENA inversions assimilate a fixed number of stations during the entire study period (from 1980–2016) for each version. We include here two versions that differ in the number of assimilated stations: JENA_s81_v3.8 (shortened as JENA_s81) and JENA_s04_v3.8 (shortened as JENA_s04). JENA_s81 has the longest validity period of 1981–2015 with temporally consistent constraints from the same set of 15 stations over the globe, while JENA_s04 has a shorter validity period from 2004 to 2015 but assimilated the largest number of sites among the JENA inversions (59 sites). Results before 2004 are available from the JENA_s04, but they are constrained by fewer stations than those within the validity period. JENA_s04 has more detailed constrains on the carbon exchanges for the later part of our study period. Also, it is relatively more comparable with the CAMS results in terms of the number of observations used. The JENA inversions have a spatial resolution of 3.75° × 5° with daily optimized fluxes. By using these inversions of very different configurations, we cover a broad range of uncertainties associated with the NBP obtained from atmospheric inversions.

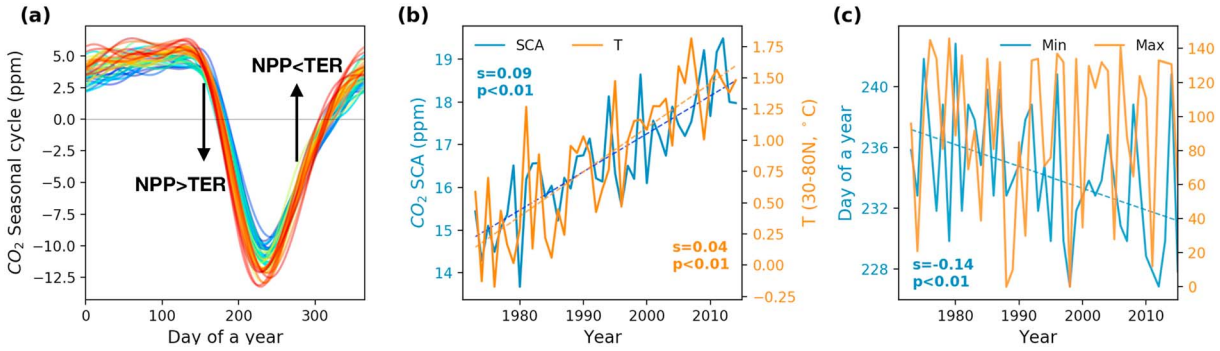

Figure 1. CO_2 seasonal cycles observed at Barrow. (a) Annual CO_2 seasonal cycles from 1971 to 2015 (color codes from blue to red). The comparison of the magnitudes of net primary productivity (NPP) and terrestrial ecosystem respiration (TER) are noted for illustrating their impacts on the CO_2 seasonal cycle. (b) Times series of the SCA (in blue) and the mean annual air temperature (in orange) in the 30–80°N zone. (c) Time series of the dates when CO_2 reaches its seasonal minimum (in blue) and maximum (in orange). The *s* means the slope of the regression line, and *p* means the *p*-value of the linear regression.

2.3. Climate Variables

Monthly air temperature (T) and precipitation (P) for the period 1973–2015 are obtained from the Climatic Research Unit TS 4.01 data sets with a spatial resolution of 0.5° (https://crudata.uea.ac.uk/cru/data/hrg/; Harris et al., 2014). All variables are averaged at the monthly scale. Regions covered by glacier all year around are masked when calculating the regional averages, for example, Greenland and high mountain ranges.

3. Temporal Changes in the SCA and its Response to Temperature Variations

Detrended CO_2 measurements at Barrow reach annual minimum values in late July/early August after a period of rapid CO_2 drawdown and then builds up gradually until December, followed by stable high CO_2 levels until the next years' spring (Figure 1a). SCA increased significantly during the past four decades with deeper and earlier CO_2 troughs ($p < 0.01$), along with the increasing trend in the mean annual NH surface air temperature (T, 30–80°N), though both have considerable interannual variations (~8% IAV for SCA and ~4% for T; Figure 1b). The timing of annual troughs showed a general advancing trend (−0.14 day/year), while no trend found for the timing of seasonal CO_2 maximum; the latter also spans a much longer temporal window so that its timing is not as clearly defined as the one of the summer minimum (Figure 1c). The rate at which SCA increases slowed down from the early 1970s to the early 1990s and started to increase again afterwards (Figure S2a). During the resumed acceleration of SCA increase, the rate of T increase slowed down (Figure S2b). The advance of the CO_2 troughs occurred mostly in the 1980–1990s, whereas the delay in its phase was found around the year 2000 (Figure S2c). CO_2 peak dates only show significant advance in the early period of the records (Figure S2d).

We further investigate the temporal variations in the year-to-year correlations between SCA and T using moving windows, within which both variables were detrended to analyze the covariations between their anomalies. The sign of the correlations between ΔSCA (the anomaly in the SCA) at Barrow and ΔT (the anomaly in the mean growing season T, April–September) in the high latitudes (60–80°N) shifted gradually from positive to negative, irrespective of the moving window length of 10, 15, or 20 years (Figure 2a). The correlation between ΔSCA and midlatitude ΔT (30–60°N) changed abruptly from positive to negative around the year 2000 with a 10-year moving window (Figure 2b). The positive correlations over the 1980s and 1990s are in line with the results of Keeling et al. (1996) and Randerson et al. (1999), while the negative correlations for the later part of the record, more specifically for the SCIAMACHY period (indicated by black crosses in Figure 2), are also in agreement with the X_{CO2} results reported by Schneising et al. (2014). A similar change of the signs from positive to negative could also be found between Barrow ΔSCA and ΔT without detrending the variables or calculating ΔT for different seasons (not shown).

Extending this analysis to stations north of 30°N with observations longer than 20 years, we find that the ΔSCA-ΔT correlations were mostly positive for the pre-2000 periods (~62% of all moving windows in all 16 stations) and became negative after the 2000s (~72%), in which ΔT is estimated for the latitudinal band

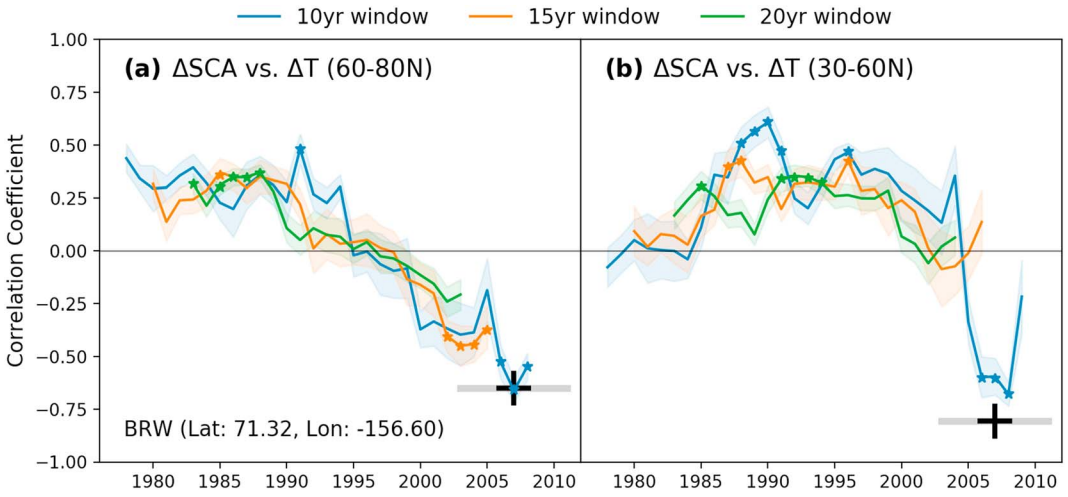

Figure 2. Change in the correlation coefficients between the year-to-year variations of SCA at Barrow (70°N) and the Northern Hemisphere air temperature over the last four decades. (a) Moving correlation between ΔSCA and ΔT in the 60–80°N zone. Both variables are detrended within the moving window; the color codes represent different window lengths, and each data point is drawn at the middle of the analyzing window; the shaded areas show the standard deviations of the correlation coefficients estimated using a bootstrap method; the colored stars mark significant correlations at the 90% confidence level; the black cross indicates the correlation coefficient over the SCIAMACHY period (2003–2011). (b) The same components as in (a) but for ΔT in the 30–60°N zone.

surrounding each station by 30°. However, only a few stations show statistically significant correlations at a 90% confidence level (4 out of 11 for the pre-2000 period and 6 out of 16 for the post-2000 period; Figure S1).

Results based on available satellite X_{CO2} retrievals for the post-2000 period are consistent with the surface measurements. An anticorrelation between SCIAMACHY ΔSCA and ΔT is found over the 30–80°N latitudinal band (2003–2011, $r = -0.7$, $p = 0.04$), similar to the results of Schneising et al. (2014). A negative correlation is also found using GOSAT, but it is not statistically significant ($r = -0.52$, $p = 0.29$). As the satellite measurements sample the interior of the continents within the 30–80°N zone, we divide it longitudinally into five subcontinents, namely, Western North America, Eastern North America, West Europe, Central Asia, and East Asia, to analyze the correlations between inland ΔSCA and ΔT. Most regions show insignificant negative ΔSCA-ΔT correlations with some divergences among the regions (Table S1). However, a short temporal record limits these analyses, in addition to the uncertainty due to sampling gaps with cloud and aerosol and limited cold season coverage. Focusing on the well-sampled growing season, Wunch et al. (2013) found that smaller magnitudes of summer X_{CO2} drawdowns are associated with higher boreal temperatures, using ground-based Total Carbon Column Observing Network (TCCON) and GOSAT observations from four northern sites for parts of the late 2000s. A smaller summer CO_2 drawdown would result in a smaller SCA assuming everything else remains unchanged, thus in line with the negative ΔSCA-ΔT correlation for this era found in this study.

4. Changing Correlations Between NBP and T in Different Seasons

SCA observed at an individual station is primarily controlled by the magnitude of the local growing season CO_2 uptake and the nongrowing season CO_2 release and the dynamics of the transport. Inversion systems integrate CO_2 observations from multiple stations (including those studied above) and have the advantage of explicitly accounting for changes in the transport, guided by meteorological reanalyses. Hence, we use spatially and temporally resolved NBP from atmospheric inversions to study the change of correlations between seasonal NBP (positive values indicate net land carbon sink) and T. The decadal changes of correlations between seasonal anomalies of NBP (ΔNBP) and temperature (ΔT) analyzed by a 10-year moving window are shown in Figure 3. Results using 15- or 20-year moving windows are qualitatively in agreement with the 10-year trends, but since they have less temporal variations by construction, they are not further described.

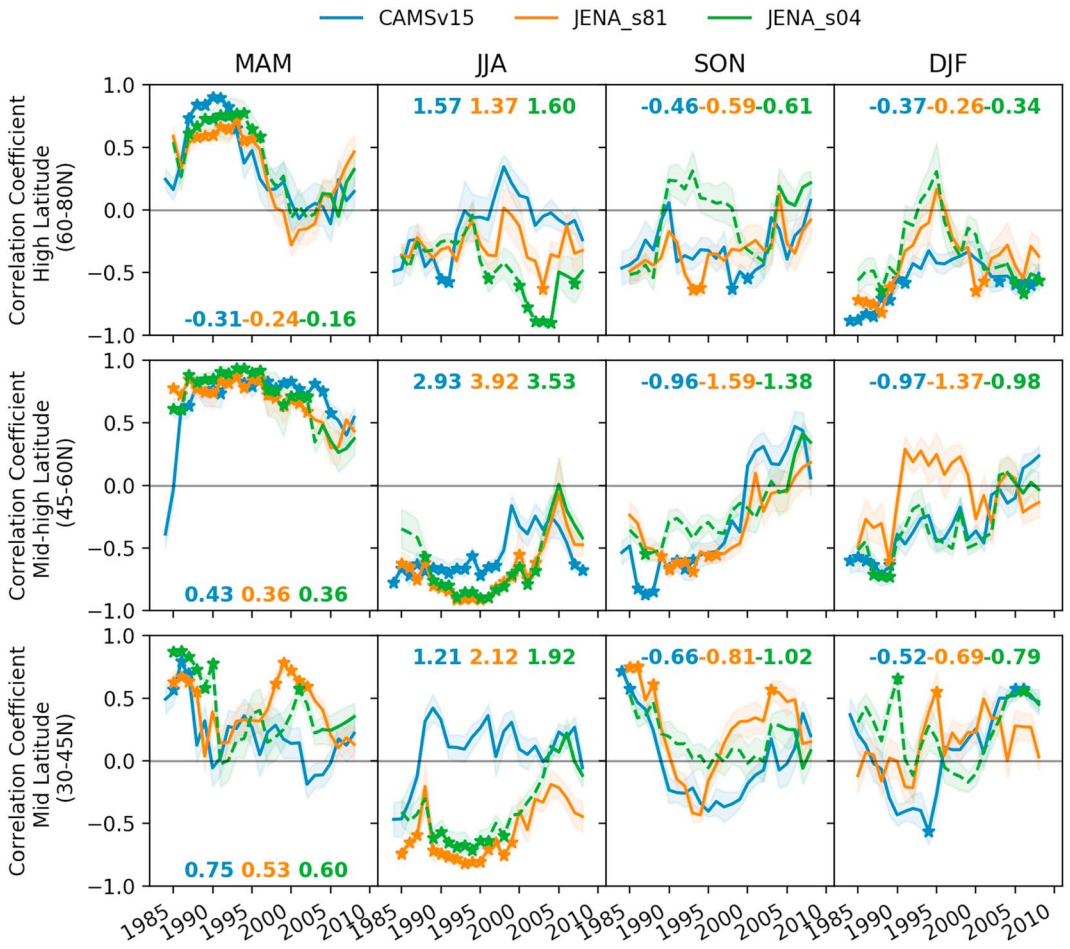

Figure 3. Moving correlations between ΔNBP and ΔT using a 10-year window. Each row presents a zonal band (midlatitude, mid-to-high latitude, and high latitude) and each column a season from spring (March–May) to winter (December–February). Both variables are detrended within the moving window, and each data point is drawn at the middle of the analyzing window. The color codes represent the three atmospheric inversions, and the shaded areas show the uncertainty of the correlation coefficients estimated using a bootstrap method; the stars mark significant correlations at the 90% confidence level. The numbers denote the multiyear average net biome productivity (NBP) estimated by the corresponding inversion product with the same color code (a positive NBP value means net land carbon uptake, a negative value means net carbon release from the land to the atmosphere). Note that for the JENA_s04 inversion, results outside its validity period 2004–2015, which does not have consistent network constraint, are shown in dashed lines.

4.1. Weakening of the Positive NBP-T Correlation in Spring

The three inversions show reasonably good agreement in the change of ΔNBP-ΔT correlations in most seasons over the three latitude bands, defined here as midlatitudes (the 30–45°N), mid-to-high latitudes (45–60°N), and high latitudes (60–80°N). Results indicate significant reductions of the positive ΔNBP-ΔT correlations in the spring (March–May) for all three zones (Figure 3, first column). The zonally integrated spring NBP is negative in the high-latitude zone 60–80°N (net carbon sources) and positive in regions 45–60°N and 30–45°N (net carbon sink; Figure S3). The decrease in the positive spring ΔNBP-ΔT correlation suggests that the effect of larger net carbon uptakes with higher spring temperatures weakens in time, most prominently in the high latitudes since the early 1990s. The decrease in NBP sensitivity to T in the mid-to-high latitudes is more gradual, emerging at a later period (after the 2000s). For the midlatitudes, there are relatively larger differences among the three inversions, possibly due to differences in the number and location of assimilated sites within this zone (see annual station map for CAMS in Chevallier, 2016) and the station distribution for the JENA_s81 in Figure S6).

Assuming that other components remain the same, the decrease in temperature sensitivity of spring carbon uptake would result in a smaller increase in SCA during warmer years. This decrease in the spring ΔNBP-ΔT correlation is in line with a recent study showing that the strong correlation between spring temperature and the spring CO_2 zero-crossing date or the magnitude of CO_2 drawdown at Barrow between May and June has disappeared in the last 17 years (1996–2012 versus 1979–1995; Piao, Liu, Wang, Peng, et al., 2017). Fu et al. (2015) also found that the response of leaf unfolding to climate warming has significantly decreased from 1980 to 2013, using field observations of the leaf unfolding dates in Europe. Our results here confirm the temporal change of NH spring temperature sensitivity at a regional scale using zonal integrated surface carbon fluxes and show that the high latitudes have the largest decrease in sensitivity and the earliest onset of change, followed by the mid-to-high latitudes.

4.2. Diminishing of the Negative NBP–T Correlation in Autumn and Winter

Another feature on which the inversions agree is the weakening of the negative ΔNBP-ΔT correlation during autumn (September–November) in the mid-to-high latitudes and, to some degree, in the high latitudes (Figure 3, third column). The seasonally integrated NBP is negative in autumn for all three zones (respiration $>$ photosynthesis, NBP being a source of CO_2 to the atmosphere). The weakening of the negative correlations between ΔNBP and ΔT in autumn suggests that higher temperatures become less associated with higher net releases of CO_2 from land in the recent decade compared to earlier periods, and thus smaller SCA during higher T. A similar weakening of the negative ΔNBP-ΔT correlations also emerged in winter in the mid-to-high latitudes and, to some extent, in the high-latitudes (Figure 3, fourth column).

These findings are counterintuitive given that net primary productivity outside the peak growing season is relatively small (NBP being negative for both seasons) and soil respiration rates are expected to increase with temperature (Bond-Lamberty & Thomson, 2010; Lloyd & Taylor, 1994), opposite to what is observed. Focusing on processes driving the uptake of CO_2, vegetation greenness has increased prominently in autumn and winter since 2000 in central and eastern Siberia, Eastern North America, and parts of Europe as shown in a recent study (see Figure 1 in Yue et al., 2017), indicating vigorous vegetation activity outside the peak growing season in the mid-to-high latitudes in the recent decades. Indeed, using normalized difference vegetation index (NDVI) observed from the Moderate Resolution Imaging Spectroradiometer instruments Collection 6 (Didan, 2015)—a proxy for vegetation greenness, we found, in general, positive correlations between ΔNDVI and ΔT in the midlatitudes and mid-to-high latitudes during autumn and winter (Figure S4). This pattern suggests that warmer temperatures could potentially contribute to higher photosynthetic uptake during autumn and winter in these latitudes. Note that winter is defined here as December to February, which may include the onset of the growing season in some midlatitudinal regions where agriculture may have significant contributions (Gray et al., 2014).

Focusing instead on the processes that release CO_2 outside the peak growing season, we note a recent study showing a significant decrease in the snow depth over the last 45 years (see Figure 1 in Kunkel et al., 2016), which could modulate the correlation between winter NBP and air temperature, particularly along the southern extent of the snow cover that has the largest relative loss. The mechanism is that snow cover acts as an insulator for the soil temperature, providing protection from extreme cold winter air temperature (Wang et al., 2016). Since soil respiration depends more on soil temperature than on air temperature (Yu et al., 2016), reduced snow depth can lead to a cooling of the topsoil temperature and thus reduce soil respiration. Yu et al. (2016) estimated that decreasing depths of snow cover reduced winter soil respiration from 1982 to 2009, accounting for ~25% of the simulated annual carbon sink increase.

In addition, soil respiration during the nongrowing season is also regulated by the carbon input of the previous growing season. In general, summer NBP is negatively correlated with T; in the 30–45°N band, temperatures among the four seasons were more tightly correlated in the pre-2000 period than in the post-2000 period (Figure S5); this could potentially contribute to some of the changes in the correlation of fall NBP-T. Along the line of covariations between different climate variables, the decoupling of variations between temperature and precipitation in the post-2000 in the midlatitudes as well as emerging drought stress could also contribute to some of the changes we observed (Figure S5). We emphasize that the response of soil respiration to changes in temperature is complex, including other physical, chemical, and biological mechanisms that control soil carbon decomposition and stabilization (Davidson & Janssens, 2006). For instance, nitrogen deposition in the temperate forest is shown to impede soil carbon decomposition in a magnitude equivalent

to the amount of carbon uptake owing to nitrogen fertilization (Janssens et al., 2010). We also note some decreasing trends in the net carbon uptake in the autumn (increases in the net CO_2 release) in the 30–45°N and 45–60°N bands prior to 2000, but these trends leveled off after 2000 (Figure S3). Further process-specific measurements and investigations are needed to address the aforementioned processes in future studies.

The results for the summer ΔNBP-ΔT correlations show larger differences among the three inversions: they agree on a general negative ΔNBP-ΔT correlation in the high and mid-to-high latitudes, but CAMS and JENA differ on the correlations in the midlatitudes. Overall, the inverse results indicate that the correlation between ΔSCA and ΔT becoming negative after the 2000s are due to the combined effect of two mechanisms: (1) weaker positive correlation between NBP uptake and positive ΔT anomalies in spring (that is, the CO_2 minimum being less pronounced in warmer years) and (2) weaker coupling between respiration emissions and positive ΔT anomalies in autumn and winter (that is, the CO_2 maximum becoming less pronounced in warmer years), with the summer NBP-T correlation being negative in general.

4.3. Spatial Distribution of Observable Changes in the NBP-T Correlation

We further analyze the spatial distribution of changes in the ΔNBP-ΔT correlation. Only the JENA_s81 inversion is used, as it is constrained by a consistent observation network for the period 1980–2015. It is more difficult to attribute the temporal variations in the ΔNBP-ΔT correlations using CAMS, given that the observational constraint in space also varies in time for this inversion. The spatial distribution of trends in the correlation coefficients that are observable by the sets of time-invariant stations in JENA_S81 is shown in Figure S6, where positive trends indicate enhanced positive correlations or reduced negative correlations, and vice versa.

At a continental scale, we find strong negative trends during the spring in the temperate regions of North America (weakening of positive correlations), while the mid-to-low latitudes showed some positive trends (enhancing of positive correlations; Figure S6a). Small negative trends were also found in the western part of temperate North America in summer suggesting enhanced negative correlations (Figure S6b). Positive trends in both midlatitudes and high latitudes of North America are found during autumn, indicating a weakening of the negative correlations (Figure S6c). In winter, contrasting patterns between the high latitudes (enhanced negative correlations) and midlatitudes (diminishing negative correlations) are found across North America (Figure S6d). The difference in the temperature sensitivity and its temporal change between the high latitude and the mid-latitude vegetation have also been noted by previous studies using the growing season NDVI (Piao et al., 2014).

In contrast, there are very few stations located in Eurasia and its outflow regions in the Pacific Ocean. The most prominent features that we observe are the positive trends in the correlations between ΔNBP and ΔT in the midlatitudes during winter (diminishing negative correlations). These spatial patterns are in line with the temporal changes of the zonal integrated fluxes and temperatures as discussed above (Figure 3). The spatial distribution of changes in the ΔNBP-ΔT correlations should be interpreted with caution, as atmospheric inversions present increasing uncertainties for smaller scales due to the limited number of observation sites, the limitations of transport models, and increasing posterior error correlations.

5. Conclusion

We analyzed the temporal changes in the year-to-year correlations between SCA and T using long-term surface CO_2 observations from 16 NH stations. Similar to the results at Barrow that show a change in the sign of the ΔSCA-ΔT correlations, most stations show positive ΔSCA-ΔT correlations for the pre-2000 periods and negative correlations for the post-2000 periods. Negative correlations for the post-2000 periods are also found using satellite X_{CO2} observations from SCIAMACHY and GOSAT. We further explored potential causes of this change in the ΔSCA-ΔT correlations using spatially and temporally resolved NBP from atmospheric inversions. The weakening of the positive spring ΔNBP-ΔT correlation (higher T, larger net C sink) would result in a reduction in the positive correlation between ΔSCA and ΔT; the shift in the negative autumn/winter ΔNBP-ΔT correlation (higher T, larger net C release) could result in a change in the ΔSCA-ΔT correlation from positive to negative as the summer ΔNBP-ΔT correlations are generally negative. The diminishing positive correlations between spring carbon uptake and temperature anomalies imply a limit to the "warmer

spring-larger carbon sink" mechanism that has driven high-latitude carbon cycle dynamics over the last half century. The negative to positive switch between fall/winter ΔNBP-ΔT, challenging the "warmer winter-larger carbon release" assumption, highlights both the complexity of the carbon processes outside the peak growing season that requires further studies, and at the same time, the resultant uncertainty arises in our ability to project future carbon-climate feedback.

Acknowledgments
All the data supporting this study can be found in the citation of the data sources. The authors thank Christian Rödenbeck for providing the JENA inversion results and helpful discussion. We acknowledge the Earth System Research Laboratory, National Oceanic and Atmospheric Administration (NOAA-ESRL) Carbon Cycle Greenhouse Gases (CCGG) group for providing the surface CO_2 measurements from various stations, with special thanks to Ed Dlugokencky and Pieter Tans for their helpful instructions regarding the data set. We thank the ESA GHG-CCI project for providing satellite X_{CO2} retrievals of IUP-Bremen University SCIAMACHY and Leicester University GOSAT. The authors are very grateful to the many people involved in the surface and satellite CO_2 observations and in the archiving of these data. We also wish to thank N. C. Parazoo for helpful comments on the manuscript. The research leading to these results has received funding from the European Research Council Synergy grant ERC-2013-SyG 610028 (IMBALANCE-P) and from the French Agence Nationale de la Recherche (ANR) Convergence Lab Changement climatique et usage des terres (CLAND).

References

Bond-Lamberty, B., & Thomson, A. (2010). Temperature-associated increases in the global soil respiration record. *Nature*, *464*(7288), 579–582. https://doi.org/10.1038/nature08930

Chevallier, F. (2016). Validation report for the inverted CO_2 fluxes, v15r2. Retrieved from http://atmosphere.copernicus.eu/sites/default/files/FileRepository/Resources/Validation-reports/Fluxes/CAMS73_2015SC1_D73.1.2_201606_Val_Inverted_CO2_Fluxes_v3.pdf

Chevallier, F., Ciais, P., Conway, T. J., Aalto, T., Anderson, B. E., Bousquet, P., et al. (2010). CO_2 surface fluxes at grid point scale estimated from a global 21 year reanalysis of atmospheric measurements. *Journal of Geophysical Research*, *115*, D21307. https://doi.org/10.1029/2010JD013887

Cogan, A. J., Boesch, H., Parker, R. J., Feng, L., Palmer, P. I., Blavier, J.-F. L., et al. (2012). Atmospheric carbon dioxide retrieved from the Greenhouse gases Observing SATellite (GOSAT): Comparison with ground-based TCCON observations and GEOS-Chem model calculations. *Journal of Geophysical Research*, *117*, D21301. https://doi.org/10.1029/2012JD018087

Davidson, E. A., & Janssens, I. A. (2006). Temperature sensitivity of soil carbon decomposition and feedbacks to climate change. *Nature*, *440*(7081), 165–173. https://doi.org/10.1038/nature04514

Didan, K. (2015). MOD13C1 MODIS/Terra Vegetation Indices 16-Day L3 Global 0.05Deg CMG V006.

Dlugokencky, E. J., Lang, P. M., Mund, J. W., Crotwell, A. M., Crotwell, M. J., & Thoning, K. W. (2017). Atmospheric carbon dioxide dry air mole fractions from the NOAA ESRL Carbon Cycle Cooperative Global Air Sampling Network, 1968–2016, Version: 2017–07-28. Retrieved from ftp://aftp.cmdl.noaa.gov/data/trace_gases/co2/flask/surface/

Forkel, M., Carvalhais, N., Rödenbeck, C., Keeling, R., Heimann, M., Thonicke, K., et al. (2016). Enhanced seasonal CO_2 exchange caused by amplified plant productivity in northern ecosystems. *Science*, *351*(6274), 696–699. https://doi.org/10.1126/science.aac4971

Fu, Y. H., Zhao, H., Piao, S., Peaucelle, M., Peng, S., Zhou, G., et al. (2015). Declining global warming effects on the phenology of spring leaf unfolding. *Nature*, *526*(7571), 104–107. https://doi.org/10.1038/nature15402

Graven, H. D., Keeling, R. F., Piper, S. C., Patra, P. K., Stephens, B. B., Wofsy, S. C., et al. (2013). Enhanced seasonal exchange of CO_2 by northern ecosystems since 1960. *Science*, *341*(6150), 1085–1089. https://doi.org/10.1126/science.1239207

Gray, J. M., Frolking, S., Kort, E. A., Ray, D. K., Kucharik, C. J., Ramankutty, N., & Friedl, M. A. (2014). Direct human influence on atmospheric CO_2 seasonality from increased cropland productivity. *Nature*, *515*(7527), 398–401. https://doi.org/10.1038/nature13957

Harris, I., Jones, P. D., Osborn, T. J., & Lister, D. H. (2014). Updated high-resolution grids of monthly climatic observations—Rhe CRU TS3.10 dataset. *International Journal of Climatology*, *34*(3), 623–642. https://doi.org/10.1002/joc.3711

Janssens, I. A., Dieleman, W., Luyssaert, S., Subke, J.-A., Reichstein, M., Ceulemans, R., et al. (2010). Reduction of forest soil respiration in response to nitrogen deposition. *Nature Geoscience*, *3*(5), 315–322. https://doi.org/10.1038/ngeo844

Keeling, C. D., Chin, J. F. S., & Whorf, T. P. (1996). Increased activity of northern vegetation inferred from atmospheric CO_2 measurements. *Nature*, *382*(6587), 146–149. https://doi.org/10.1038/382146a0

Kunkel, K. E., Robinson, D. A., Champion, S., Yin, X., Estilow, T., & Frankson, R. M. (2016). Trends and extremes in northern hemisphere snow characteristics. *Current Climate Change Reports*, *2*(2), 65–73. https://doi.org/10.1007/s40641-016-0036-8

Lloyd, J., & Taylor, J. A. (1994). On the temperature dependence of soil respiration. *Functional Ecology*, *8*(3), 315. https://doi.org/10.2307/2389824

Parazoo, N. C., Commane, R., Wofsy, S. C., Koven, C. D., Sweeney, C., Lawrence, D. M., et al. (2016). Detecting regional patterns of changing CO_2 flux in Alaska. *Proceedings of the National Academy of Sciences of the United States of America*, *113*(28), 7733–7738. https://doi.org/10.1073/pnas.1601085113

Peters, W., Jacobson, A. R., Sweeney, C., Andrews, A. E., Conway, T. J., Masarie, K., et al. (2007). An atmospheric perspective on North American carbon dioxide exchange: CarbonTracker. *Proceedings of the National Academy of Sciences of the United States of America*, *104*(48), 18,925–18,930. https://doi.org/10.1073/pnas.0708986104

Piao, S., Ciais, P., Friedlingstein, P., Peylin, P., Reichstein, M., Luyssaert, S., et al. (2008). Net carbon dioxide losses of northern ecosystems in response to autumn warming. *Nature*, *451*(7174), 49–52. https://doi.org/10.1038/nature06444

Piao, S., Liu, Z., Wang, T., Peng, S., Ciais, P., Huang, M., et al. (2017). Weakening temperature control on the interannual variations of spring carbon uptake across northern lands. *Nature Climate Change*, *7*(5), 359–363. https://doi.org/10.1038/nclimate3277

Piao, S., Liu, Z., Wang, Y., Ciais, P., Yao, Y., Peng, S., et al. (2017). On the causes of trends in the seasonal amplitude of atmospheric CO_2. *Global Change Biology*, *24*(2), 608–616. https://doi.org/10.1111/gcb.13909

Piao, S., Nan, H., Huntingford, C., Ciais, P., Friedlingstein, P., Sitch, S., et al. (2014). Evidence for a weakening relationship between interannual temperature variability and northern vegetation activity. *Nature Communications*, *5*, 5018. https://doi.org/10.1038/ncomms6018

Randerson, J. T., Field, C. B., Fung, I. Y., & Tans, P. P. (1999). Increases in early season ecosystem uptake explain recent changes in the seasonal cycle of atmospheric CO_2 at high northern latitudes. *Geophysical Research Letters*, *26*, 2765–2768. https://doi.org/10.1029/1999GL900500

Randerson, J. T., Thompson, M. V., Conway, T. J., Fung, I. Y., & Field, C. B. (1997). The contribution of terrestrial sources and sinks to trends in the seasonal cycle of atmospheric carbon dioxide. *Global Biogeochemical Cycles*, *11*, 535–560. https://doi.org/10.1029/97GB02268

Reuter, M., Bovensmann, H., Buchwitz, M., Burrows, J. P., Connor, B. J., Deutscher, N. M., et al. (2011). Retrieval of atmospheric CO_2 with enhanced accuracy and precision from SCIAMACHY: Validation with FTS measurements and comparison with model results. *Journal of Geophysical Research*, *116*, D04301. https://doi.org/10.1029/2010JD015047

Rödenbeck, C., Houweling, S., Gloor, M., & Heimann, M. (2003). CO_2 flux history 1982–2001 inferred from atmospheric data using a global inversion of atmospheric transport. *Atmospheric Chemistry and Physics*, *3*(6), 1919–1964. https://doi.org/10.5194/acp-3-1919-2003

Schneising, O., Reuter, M., Buchwitz, M., Heymann, J., Bovensmann, H., & Burrows, J. P. (2014). Terrestrial carbon sink observed from space: Variation of growth rates and seasonal cycle amplitudes in response to interannual surface temperature variability. *Atmospheric Chemistry and Physics*, *14*(1), 133–141. https://doi.org/10.5194/acp-14-133-2014

Thoning, K., Tans, P., & Komhyr, W. (1989). Atmospheric carbon dioxide at Mauna Loa Observatory. II—Analysis of the NOAA GMCC data, 1974–1985. *Journal of Geophysical Research*, *94*, 8549–8565. https://doi.org/10.1029/JD094iD06p08549

Wang, W., Rinke, A., Moore, J. C., Ji, D., Cui, X., Peng, S., et al. (2016). Evaluation of air–soil temperature relationships simulated by land surface models during winter across the permafrost region. *The Cryosphere*, *10*(4), 1721–1737. https://doi.org/10.5194/tc-10-1721-2016

Wunch, D., Wennberg, P. O., Messerschmidt, J., Parazoo, N. C., Toon, G. C., Deutscher, N. M., et al. (2013). The covariation of Northern Hemisphere summertime CO_2 with surface temperature in boreal regions. *Atmospheric Chemistry and Physics*, *13*(18), 9447–9459. https://doi.org/10.5194/acp-13-9447-2013

Yu, Z., Wang, J., Liu, S., Piao, S., Ciais, P., Running, S. W., et al. (2016). Decrease in winter respiration explains 25% of the annual northern forest carbon sink enhancement over the last 30 years. *Global Ecology and Biogeography*, *25*(5), 586–595. https://doi.org/10.1111/geb.12441

Yue, C., Ciais, P., Bastos, A., Chevallier, F., Yin, Y., Rödenbeck, C., & Park, T. (2017). Vegetation greenness and land carbon-flux anomalies associated with climate variations: A focus on the year 2015. *Atmospheric Chemistry and Physics*, *17*(22), 13,903–13,919. https://doi.org/10.5194/acp-17-13903-2017

Zhu, Z., Piao, S., Myneni, R. B., Huang, M., Zeng, Z., Canadell, J. G., et al. (2016). Greening of the Earth and its drivers. *Nature Climate Change*, *6*(8), 791–795. https://doi.org/10.1038/nclimate3004